

Critical Point-Finding Methods Reveal Gradient-Flat Regions of Deep Network Losses

*Charles G. Frye^{1,2}, James Simon^{1,3}, Neha S. Wadia^{1,4}, Andrew Ligeralde^{1,4}, †Michael R. DeWeese^{1,2,3,4}, and †Kristofer E. Bouchard^{1,2,5,6}

¹Redwood Center for Theoretical Neuroscience, University of California, Berkeley, CA, USA

²Helen Wills Neuroscience Institute, University of California, Berkeley, CA, USA

³Department of Physics, University of California, Berkeley, CA, USA

⁴Biophysics Graduate Group, University of California, Berkeley, CA, USA

⁵Biological Systems and Engineering Division, Lawrence Berkeley National Lab, Berkeley, CA, USA

⁶Computational Research Division, Lawrence Berkeley National Lab, Berkeley, CA, USA

Abstract

Despite the fact that the loss functions of deep neural networks are highly non-convex, gradient-based optimization algorithms converge to approximately the same performance from many random initial points. One thread of work has focused on explaining this phenomenon by characterizing the local curvature near critical points of the loss function, where the gradients are near zero, and demonstrating that neural network losses enjoy a no-bad-local-minima property and an abundance of saddle points. We report here that the methods used to find these putative critical points suffer from a bad local minima problem of their own: they often converge to or pass through regions where the gradient norm has a stationary point. We call these *gradient-flat regions*, since they arise when the gradient is approximately in the kernel of the Hessian, such that the loss is locally approximately linear, or flat, in the direction of the gradient. We describe how the presence of these regions necessitates care in both interpreting past results that claimed to find critical points of neural network losses and in designing second-order methods for optimizing neural networks.

1 Introduction

Large neural networks are surprisingly easy to optimize [46], despite the substantial non-convexity of the loss as a function of the parameters [19]. In particular, it is usually found that changing the random initialization has no effect on performance, even though it can change the model learned by gradient-based optimization methods [17]. Understanding the cause of trainability from random initial conditions is critical for the development of new architectures and optimization methods, which must otherwise just hope to retain this favorable property based on heuristics.

One possible explanation for this phenomenon is based on the stationary points of gradient-based optimization methods. These methods are stationary when the gradient of the loss function is 0, at the *critical points* of the loss. Critical points are classified by their Morse index, or the degree of local negative curvature (i.e., the relative number of dimensions in parameter space along which the curvature is negative). Since, among all critical points, gradient descent methods only converge to those points with index 0 [29], which includes local minima, it has been argued that large neural networks are easy to train because their loss functions for many problems only have local minima at values of the loss close to or at the global optimum. This is known as the “no-bad-local-minima” property. Previous work [11, 39] has reported numerical evidence for a convex relationship between index and loss that supports the hypothesis that neural network loss functions have the no-bad-local-minima property: for low values of the loss, only low values of the index were observed, whereas for high values of the loss, only high values of the index were observed. However, more recent theoretical work has indicated that there are in fact bad local minima on neural network losses in almost all cases [12].

*To whom correspondence should be addressed: charlesfrye@berkeley.edu

†These authors contributed equally to the work.

The validity of the numerical results depends on the validity of the critical point-finding algorithms, and the second-order critical point-finding algorithms used in [11] and [39] are not in fact guaranteed to find critical points in the case where the Hessian is singular. In this case, the second-order information used by these critical point-finding methods becomes unreliable.

Neural network loss Hessians are typically highly singular [44], and poor behavior of Newton-type critical point-finding methods has been reported in the neural network case [10], casting doubt on the completeness and accuracy of the results in [11] and [39]. [16] verified that second-order methods can in fact find high-quality approximate critical points for linear neural networks, for which the analytical form of the critical points is known [2], providing ground truth. In particular, the two phase convergence pattern predicted by the classical analysis of Newton methods [36] is evident: a linear phase followed a short, local supralinear phase (Fig. 1A). The supralinear convergence is visible in the “cliffs” in the blue traces in Fig. 1A, where the convergence rate suddenly improves. With a sufficiently strict cut-off on the gradient norms, the correct loss-index relationship obtained analytically (Fig. 1B, gray points) is shared by the points obtained numerically (Fig. 1B, light blue points). With an insufficiently strict cutoff, the loss-index relationship implied by the observed points is far from the truth (Fig. 1B, dark red points)

Unfortunately, good performance on linear networks does not guarantee good performance on non-linear networks. When applied to a non-linear network, even with the same data, the behavior of these Newton methods changes dramatically for the worse (Fig. 1C). No runs exhibit supralinear convergence and the gradient norms at termination are many orders of magnitude larger. These are not the signatures of a method converging to a critical point, even though gradient norms are sometimes still under the thresholds reported in [39] and [16] (no threshold reported in [11]). This makes it difficult to determine whether the putative loss-index relationship measured from these critical points (Fig. 1D) accurately reflects the loss-index relationship at the true critical points of the loss function.

In this paper, we identify a major cause of this failure for second-order critical point-finding methods: *gradient-flat regions*, where the gradient is approximately in the kernel of the Hessian. In these regions, the loss function is locally approximately linear along the direction of the gradient, whether or not the gradient is itself small, as would be the case near a true critical point. We first define gradient-flatness (Sec. 2.1) and explain, with a low-dimensional example (Sec. 2.2), why it is problematic for second-order methods: gradient-flat points can be “bad local minima” for the problem of finding critical points. We then provide evidence that gradient-flat regions are encountered when applying the Newton-MR algorithm to a deep neural network loss (Sec. 3, Appendix A.5). Furthermore, we show that, though gradient-flat regions need not contain actual critical points, the loss-index relationship looks strikingly similar to that reported in [11] and [39], suggesting that these previous studies may have found gradient-flat regions, not critical points. Finally, we note the implications of gradient-flatness for the design of second-order methods for use in optimizing neural networks: in the presence of gradient-flatness, approximate second-order methods, like K-FAC [32] and Adam [26] may be preferable to exact second-order methods even without taking computational cost into account.

2 Gradient-Flat Points are Stationary Points for Second-Order Methods

In this section, we introduce and define gradient-flat points and explain why they are problematic for second-order critical point-finding methods, with the help of a low-dimensional example to build intuition. In numerical settings and in high dimensions, approximately gradient-flat points are also important, and so we define a quantitative index of gradient-flatness based on the residual norm of the Newton update. Connected sets of these numerically gradient-flat points are gradient-flat regions, which cause trouble for second-order critical point-finding methods.

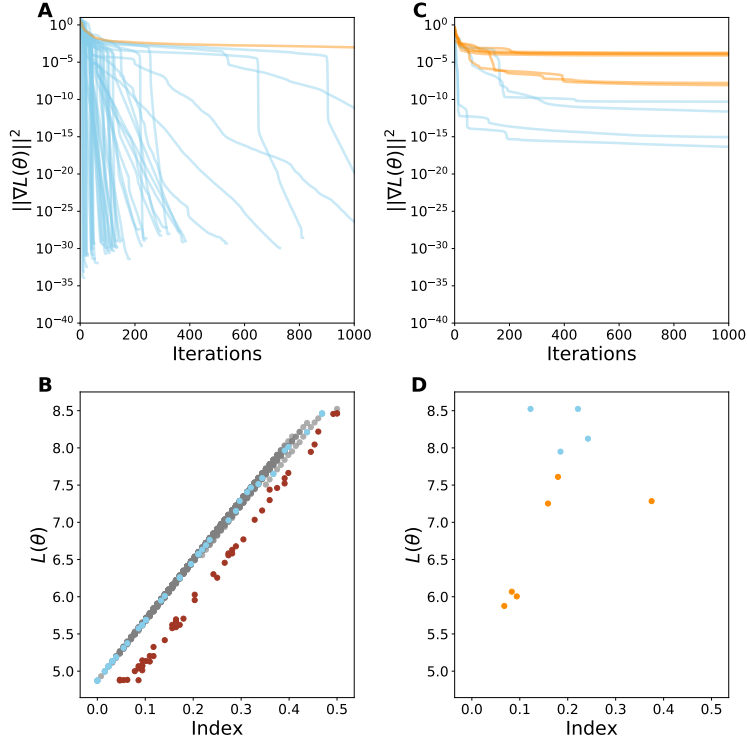


Figure 1: **Newton Methods that Find Critical Points on a Linear Network Fail on a Non-Linear Network.** **A-B:** Newton-MR on a linear autoencoder applied to multivariate Gaussian data, as in [16]. *A:* Squared gradient norms of the loss L , as a function of the parameters θ , across iterations of Newton-MR, colored by whether, after the first of early termination or 1000 epochs, squared gradient norms are below $1e-10$ (blue) or not (orange). *B:* The loss and Morse index of putative and actual critical points, with ground truth. The Morse index is defined as the fraction of negative eigenvalues. Analytically-derived critical points in gray, points from the end of runs that terminate below a squared gradient norm of $1e-10$ in light blue, and points from trajectories stopped early, once they pass a squared gradient norm of $1e-2$, in dark red. **C-D:** As in *A-B*, on the same network architecture and data, but with Swish [42] non-linear activations instead of identity activations. *D:* Loss and Morse index of putative critical points. Points with squared gradient norm above $1e-10$ in orange, those below $1e-10$ in blue. Analytical expressions for critical points are not available for this non-linear network.

2.1 At Gradient-Flat Points, the Gradient Lies in the Hessian’s Kernel

Critical points are of interest because they are points where the first-order approximation of a function f at a point¹ $x + \delta$ based on the local information at x

$$f(x + \delta) \approx f(x) + \nabla f(x)^\top \delta \quad (1)$$

is constant, indicating that they are the stationary points of first-order optimization algorithms like gradient descent and its accelerated variants. By stationary point, we mean a point at which the proposed updates of an optimization algorithm are zero. Stationary points need not be points to which the algorithm converges. For example, gradient descent almost surely only converges to critical points with index 0 [29, 23], even though its stationary points include saddle points and maxima. However, the curvature properties of non-minimal stationary points show up in proofs of the convergence rates of first order optimizers, e.g. [23, 25, 24], and so knowledge of their properties can guide algorithm design.

In searching for critical points, it is common to use a linear approximation to the behavior of the gradient at a point $x + p$ given the local information at a point x

$$\nabla f(x + p) \approx \nabla f(x) + \nabla^2 f(x) p \quad (2)$$

Because these methods rely on a quadratic approximation of the original function f , represented by the Hessian matrix of second partial derivatives, we call them second-order critical point-finding methods.

¹Note that, for a neural network loss function, the variable we take the gradient with respect to, here x , is the vector of parameters, θ , not the data, which is often denoted with an x .

The approximation on the right-hand side is constant whenever p is an element of $\ker \nabla^2 f(x)$, where $\ker M$ is notation for the kernel of a matrix M — the subspace that M maps to 0. When $\nabla^2 f(x)$ is non-singular, this is only satisfied when p is 0, so if we can define an update rule such that $p = 0$ iff $\nabla f(x) = 0$, then, for non-singular Hessians, we can be sure that our method is stationary only at critical points.

In a Newton-type method, we achieve this by selecting our step by solving for the zeroes of this linear approximation, i.e. the Newton system,

$$0 = \nabla f(x) + \nabla^2 f(x) p$$

which has solution

$$p = -\nabla^2 f(x)^+ \nabla f(x)$$

where the matrix M^+ is the Moore-Penrose pseudoinverse of the matrix M , obtained by performing the singular value decomposition, inverting the non-zero singular values, and recomposing the SVD matrices in reverse order. The Newton update p is zero iff $\nabla f(x)$ is 0 for a non-singular Hessian, for which the pseudo-inverse is simply the inverse. For a singular Hessian, the update p is zero iff $\nabla f(x)$ is in the kernel of the pseudoinverse. Note that if the Hessian is constant as a function of x , the linear model of the gradient is exact and this algorithm converges in a single step.

Within the vicinity of a critical point, this algorithm converges extremely quickly [36], but the guarantee of convergence is strictly local. Practical Newton methods in both convex optimization [5] and non-linear equation solving [36, 22] often compare multiple possible choices of p and select the best one according to a “merit function” applied to the gradients which has a global minimum for each critical point. Such algorithms have broader guarantees of global convergence. A common choice for merit function is the squared norm,

$$g(x) = \frac{1}{2} \|\nabla f(x)\|^2$$

In gradient norm minimization [33], we optimize this merit function directly. The gradients of this method are

$$\nabla g(x) = \nabla^2 f(x) \nabla f(x)$$

As with Newton methods, in the invertible case the updates are zero iff $\nabla f(x)$ is 0. In the singular case, the updates are zero if the gradient is in the Hessian’s kernel. Because this method is framed as the minimization of a scalar function, it is compatible with first-order optimization methods, which are more commonly implemented and better supported in neural network libraries.

However, neural network Hessians are generally singular, especially in the overparameterized case [44, 18], meaning the kernel is non-trivial, and so neither class of methods can guarantee convergence to critical points. Newton’s method can diverge, oscillate, or behave chaotically [20]. The addition of merit function-based upgrades can remove these behaviors, but it cannot guarantee convergence to critical points [41, 20]. The gradient norm minimization method described in [39] was previously proposed and this flaw pointed out twice in the field of chemical physics — once in the 1970s (proposed [33], critiqued [8]) and again in the 2000s (proposed simultaneously [1, 6], critiqued [13]).

What are the stationary points, besides critical points, for these two method classes in the case of singular Hessians? It would seem at first that they are different: for gradient norm minimization, when the gradient is in the Hessian’s kernel; for Newton-type methods, when the gradient is in the Hessian’s pseudoinverse’s kernel. In fact, however, these conditions are identical, due to the Hessian’s symmetry², and so both algorithms share a broad class of stationary points.

These stationary points have been identified previously, but nomenclature is not standard: Doye and Wales, studying gradient norm minimization, call them *non-stationary points* [13], since they are non-stationary with respect to the function f , while Byrd et al., studying Newton methods, call them *stationary points* [7], since they are stationary with respect to the merit function g . To avoid confusion between these incommensurate conventions or with the stationary points of the function f , we call a point where the gradient lies in the kernel of the Hessian a *gradient-flat* point. This name was chosen because a function is *flat* when its Hessian is 0, meaning every direction is in the kernel, and so it is locally flat around a

² Indeed, the kernel of the pseudo-inverse is equal to the kernel of transpose, as can be seen from the singular value decomposition, and the Hessian is equal to its transpose because it is symmetric. See [45].

point in a given direction whenever that direction is in the kernel of the Hessian at that point. Note that, because $0 \in \ker$ for all matrices, every critical point is also a gradient-flat point, but the reverse is not true. When we wish to explicitly refer to gradient-flat points which are not critical points, we will call them *strict* gradient-flat points. At a strict gradient-flat point, the function is, along the direction of the gradient, locally linear up to second order.

There is an alternative view of gradient-flat points based on the squared gradient norm merit function. All gradient-flat points are stationary points of the gradient norm, which may in principle be local minima, maxima, or saddles, while the global minima of the gradient norm are critical points. When they are local minima of the gradient norm, they can be targets of convergence for methods that use first-order approximations of the gradient map, as in gradient norm minimization and in Newton-type methods. Strict gradient-flat points, then, can be “bad local minima” of the gradient norm, and therefore prevent the convergence of second-order root-finding methods to critical points, just as bad local minima of the loss function can prevent convergence of first-order optimization methods to global optima.

Note that Newton methods cannot be demonstrated to converge only to gradient-flat points [41]. Furthermore, Newton convergence can be substantially slowed when even a small fraction of the gradient is in the kernel [20]. Below we will see that, while a Newton method applied to a neural network loss sometimes converges to and almost always encounters strict gradient-flat points, the final iterate is not always either a strict gradient-flat point or a critical point.

2.2 Convergence to Gradient-Flat Points Occurs in a Low-Dimensional Quartic Example

The difficulties that gradient-flat points pose for Newton methods can be demonstrated with a polynomial example in two dimensions, plotted in Fig. 2A. Below, we will characterize the strict gradient-flat (orange) and critical (blue) points of this function (Fig. 2A). Then, we will observe the behavior of a practical Newton method applied to it (Fig. 2B-C) and note similarities to the results in Fig. 1. We will use this simple, low-dimensional example to demonstrate principles useful for understanding the results of applying second-order critical point-finding methods to more complex, higher-dimensional neural network losses.

As our model function, we choose

$$f(x, y) = 1/4x^4 - 3x^2 + 9x + 0.9y^4 + 5y^2 + 40 \tag{3}$$

It is plotted in Fig. 2A, middle panel. This quartic function has two affine subspaces of points with non-trivial Hessian kernel, defined by $[\pm\sqrt{2}, y]$. The kernel points along the x direction, and so is orthogonal to this affine subspace at every point. As a function of y , f is convex, with one-dimensional minimizers at $y = 0$. The strict gradient-flat points occur at the intersections of these two sets: one strict gradient-flat point at $[\sqrt{2}, 0]$, which is a local minimum of the gradient norm, and one at $[-\sqrt{2}, 0]$, which is a saddle of the same (Fig. 2A, orange points, all panels). In the vicinity of these points, the gradient is, to first order, constant along the x -axis, and so the function is locally linear or flat. These points are gradient-flat but neither is a critical point of f . The only critical point is located at the minimum of the polynomial, at $[-3, 0]$ (Fig. 2A, blue point, all panels), which is also a global minimum of the gradient norm. The affine subspace that passes through $[-\sqrt{2}, 0]$ divides the space into two basins of attraction, loosely defined, for second-order methods: one, with initial x -coordinate $x_0 < -\sqrt{2}$, for the critical point of f and the other for the strict gradient-flat point. Note that the vector field in the middle panel shows update directions for the pure Newton method, which can behave extremely poorly in the vicinity of singularities [41, 20], often oscillating and converging very slowly or diverging.

Practical Newton methods use techniques like damping and line search to improve behavior [22]. To determine how a practical Newton method behaves on this function, we focus on the case of Newton-MR [43], which uses the MR-QLP [9] solver³ to compute the Newton update and back-tracking line search with the squared gradient norm merit function to select the step size. Pseudocode for this algorithm is provided in Appendix A.3. This method was found to perform better than a damped Newton method and gradient norm minimization on finding the critical points of a linear autoencoder in [16]. Results are qualitatively similar for damped Newton methods with a squared gradient norm merit function.

³MR-QLP, short for MINRES-QLP, is a Krylov subspace method akin to conjugate gradient but specialized to the symmetric, indefinite and ill-conditioned case, which makes it well-suited to this problem and to neural network losses.

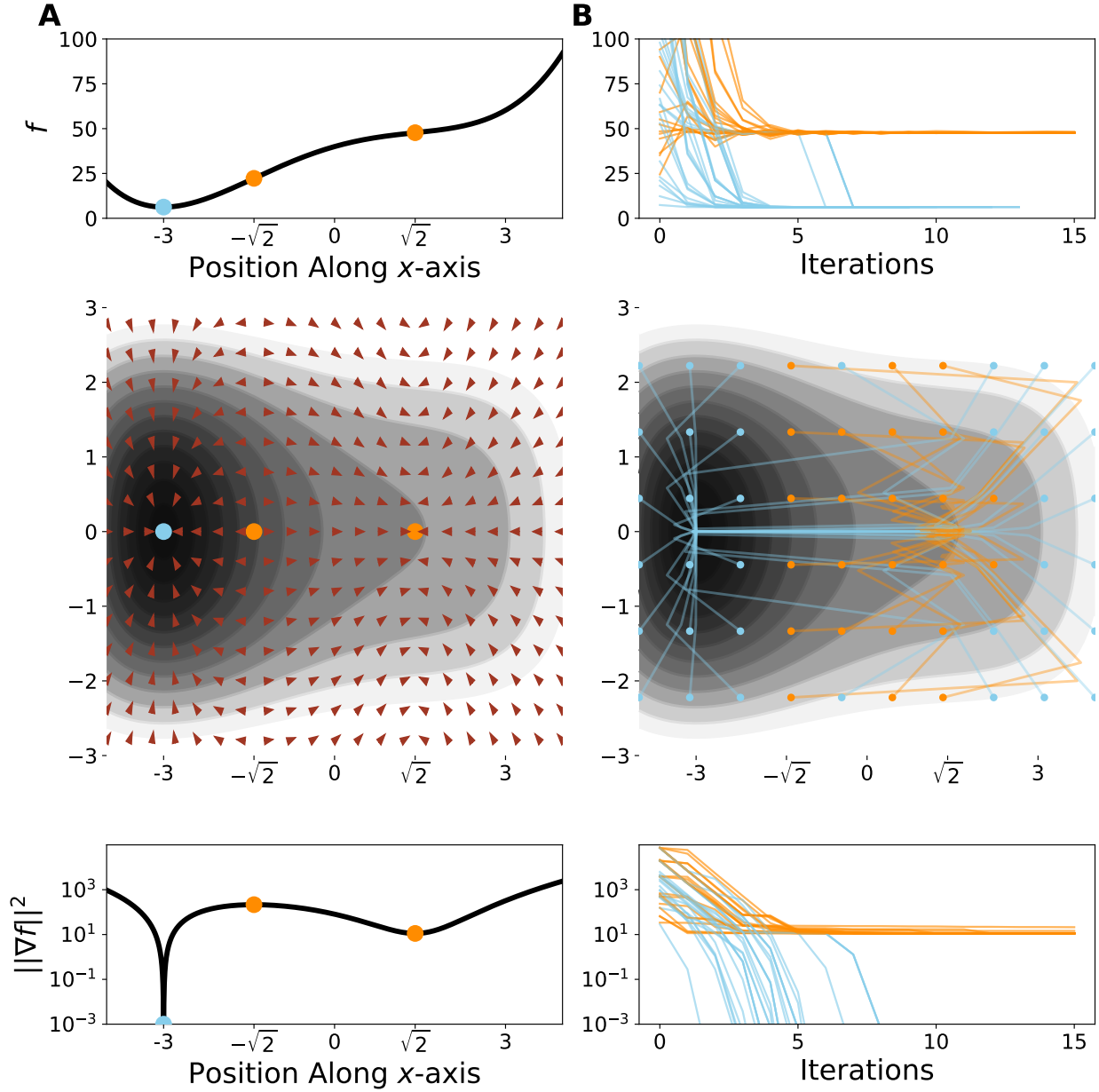


Figure 2: **Stationarity of and Convergence to a Strict Gradient-Flat Point on a Quartic Function.** **A:** Critical and strict gradient-flat points of quartic $f(x, y)$ (defined in Eqn. 3). Middle panel: $f(x, y)$ plotted in color black, low values; white, high values), along with the direction of the Newton update p as a (notably non-smooth) vector field (red). Stationary points of the squared gradient norm merit function g are indicated: strict gradient-flat points in orange, the critical point in blue. Top and bottom panels: The value (top) and squared gradient norm (bottom) of f as a function of x value with y fixed at 0. The x axis is shared between panels. **B:** Performance and trajectories of Newton-MR [43] on Eqn. 3. Runs that terminate near a strict gradient-flat point are in orange, while those that terminate near a critical point are in blue. Middle panel: Trajectories of Newton-MR laid over $f(x, y)$. x and y axes are shared with the middle panel of A. Initial values indicated with scatter points. Top and bottom panels: Function values (top) and squared gradient norms (bottom) of Newton-MR trajectories as a function of iteration. The x axis is shared between panels.

The results of applying Newton-MR to Eqn. 3 are shown in Fig. 2B. The gradient-flat point is attracting for some trajectories (orange), while the critical point is attracting for others (blue). For trajectories that approach the strict gradient-flat point, the gradient norm does not converge to 0, but converges to a non-zero value near 10 (orange trajectories; Fig. 2B, bottom panel). This value is typically several orders of magnitude lower than the initial point, and so would appear to be close to 0 on a linear scale that includes the gradient norm of the initial point. Since log-scaling of loss functions is uncommon in machine learning, as losses do not always have minima at 0, second-order methods approaching gradient-flat points can appear to converge to critical points if typical methods for visually assessing convergence are used.

There are two interesting and atypical behaviors worth noting. First, the trajectories tend to oscillate in the vicinity of the gradient-flat point and converge more slowly (Fig. 2B, middle panel, orange lines). Updates from points close to the affine subspace where the Hessian has a kernel, and so which have an approximate kernel themselves, sometimes jump to points where the Hessian doesn't have an approximate kernel. This suggests that, when converging towards a gradient-flat point, the degree of flatness will change iteration by iteration. Second, some trajectories begin in the nominal basin of attraction of the gradient-flat point but converge to the critical point (Fig. 2B, middle panel, blue points with x -coordinate $> -\sqrt{2}$). This is because the combination of back-tracking line search and large proposed step sizes means that occasionally, very large steps can be taken, based on non-local features of the function. Indeed, back-tracking line search is a limited form of global optimization and the ability of line searches to change convergence behaviors predicted from local properties on nonconvex problems is known [36]. Since the back-tracking line search is based on the gradient norm, the basin of attraction for the true critical point, which has a lower gradient norm than the gradient-flat point, is much enlarged relative to that for the gradient-flat point. This suggests that Newton methods using the gradient norm merit function will be biased towards finding gradient-flat points that also have low gradient norm.

2.3 Approximate Gradient-Flat Points and Gradient-Flat Regions

Analytical arguments focus on exactly gradient-flat points, where the Hessian has an exact kernel and the gradient is entirely within it. In numerical settings, it is almost certain no matrix will have an exact kernel, due to rounding error. For the same reason, the computed gradient vector will generically not lie entirely within the exact or approximate kernel. However, numerical implementations of second-order methods will struggle even when there is no exact kernel or when the gradient is only partly in it, and so a numerical index of flatness is required. This is analogous to the requirement to specify a tolerance for the norm of the gradient when deciding whether to consider a point an approximate critical point or not.

We quantify the degree of gradient-flatness of a point by means of the *relative residual norm* (r) and the *relative co-kernel residual norm* (r_H) for the Newton update direction p . The vector p is an inexact solution to the Newton system $Hp + g = 0$, where H and g are the current iterate's Hessian and gradient. The residual is equal to $Hp + g$, and the smaller its norm, the better p is as a solution. The co-kernel residual is equal to the Hessian times the residual, and so ignores any component in the kernel of the Hessian. Its norm quantifies the quality of an inexact Newton solution in the case that the gradient lies partly in the Hessian kernel, the unsatisfiable case, where $Hp \neq -g$ for any p . When the residual is large but the co-kernel residual is small (norms near 1 and 0, respectively, following suitable normalization), then we are at a point where the gradient is almost entirely in the kernel of the Hessian: an approximate gradient-flat point. In the results below, we consider a point approximately gradient-flat when the value of r_H is below $5e-4$ while the value of r is above 0.9. See Appendix A.4 for definitions and details. We emphasize that numerical issues for second-order methods can arise even when the degree of gradient-flatness is small.

Under this relaxed definition of gradient-flatness, there will be a neighborhood of approximate gradient-flat points around a strict, exact gradient-flat point for functions with Lipschitz-smooth gradients and Hessians. Furthermore, there might be connected sets of non-null Lebesgue measure which all satisfy the approximate gradient-flatness condition but none of which satisfy the exact gradient-flatness condition. We call both of these *gradient-flat regions*.

There are multiple reasonable numerical indices of flatness besides the definition above. For example, the Hessian-gradient regularity condition in [43], which is used to prove convergence of Newton-MR, would suggest creating a basis for the approximate kernel of the Hessian and projecting the gradient onto it. Alternatively, one could compute the Rayleigh quotient of the gradient with respect to the Hessian. Our

method has the advantage of being computed as part of the Newton-MR algorithm. It furthermore avoids diagonalizing the Hessian or the specification of an arbitrary eigenvalue cutoff. The Rayleigh quotient can be computed with only one Hessian-vector product, plus several vector-vector products, so it might be a superior choice for larger problems where computing a high-quality inexact Newton step is computationally infeasible.

3 Gradient-Flat Regions are Common on Deep Network Losses

To determine whether gradient-flat regions are responsible for the poor behavior of Newton methods on deep neural network (DNN) losses demonstrated in Fig. 1, we applied Newton-MR to the loss of a small, two hidden layer fully-connected autoencoder trained on 10k MNIST images downsized to 4x4, similar to the downsized datasets in [11, 39]. We found similar results on a fully-connected classifier trained on the same MNIST images via the cross-entropy loss (see Appendix A.5) and another classifier trained on a very small subset of 50 randomly-labeled MNIST images, as in [47] (see Appendix A.6). We focused on Newton-MR because we found that a damped Newton method like that in [11] performed poorly, as reported for the XOR problem in [10], and furthermore that there was insufficient detail to replicate [11] exactly. We denote the network losses by L and the parameters by θ . See Appendix A.1 for details on the networks and datasets and Appendix A.2 for details on the critical point-finding experiments.

Gradient norms for the first 100 iterations appear in Fig. 3A. As in the non-linear autoencoder applied to the multivariate Gaussian data (Fig. 1C), we found that, after 500 iterations, all of the runs had squared gradient norms over 10 orders of magnitude greater than the typical values observed after convergence in the linear case ($1e-30$, Fig. 1A). 14% of runs terminated with squared gradient norm below the cutoff in [16] and so found likely critical points (blue). Twice as many runs terminated above that cutoff but terminated in a gradient-flat region (28%, orange), while the remainder were above the cutoff but were not in a gradient-flat region at the final iteration (black).

The relative residual norm for the Newton solution, r , is an index of gradient-flatness; see Sec. 2.3 and Appendix A.4 for details. The values of r for every iteration of Newton-MR are shown for three representative traces in Fig. 3B. In the top trace, r is close to 0, indicating that the iterates are not in a gradient-flat region ($r \ll 0.9$, black). Newton methods can be substantially slowed when even a small fraction of the gradient is in the kernel [20] and can converge to points that are not gradient-flat [7]. By contrast, in the middle trace (orange), the value of r approaches 1, indicating that almost the entirety of the gradient is in the kernel. This run terminated in a gradient-flat region, at effectively an exactly gradient-flat point. Further, the squared gradient norm at 500 iterations, $2e-5$, is five orders of magnitude higher than the cutoff, $1e-10$. This is smaller than the minimum observed during optimization of this loss (squared gradient norms between $1e-4$ and $5e1$), indicating the presence of non-critical gradient-flat regions with very low gradient norm. Critical point-finding methods that disqualify points on the basis of their norm will both converge to and accept these points, even though they need not be near true critical points. In the bottom trace (blue), the behavior of r is the same, while the gradient norm drops much lower, to $3e-13$, suggesting convergence to a gradient-flat region around a critical point that has an approximately singular Hessian.

Not all traces exhibit such simple behavior for the value of r . In many traces, the value of r oscillates from values close to 1 to middling values, indicating that the algorithm is bouncing in and out of one or more gradient-flat regions (see Appendix A.5 for examples, on a classifier). This can occur when the final target of convergence given infinite iterations is a gradient-flat point, as in the example in Sec. 2.2.

We found that 99 of 100 traces included a point where at least half of the gradient was in the kernel, according to our residual measure, while 89% of traces included a point that had a residual greater than 0.9, and 50% included a point with $r > 0.99$ (Fig. 3C, bottom). This demonstrates that there are many regions of substantive gradient-flatness, in which second-order critical point-finding methods could be substantively slowed.

The original purpose of applying these critical point-finding methods was to determine whether the no-bad-local-minima property held for this loss function, and more broadly to characterize the relationship at the critical points between the loss and the local curvature, summarized via the Morse index. If we look at either the points found after 500 iterations (results not shown; see Appendix A.5 for an example on a classifier) or the iterates with the highest gradient-flatness (Fig. 3D), we find that the qualitative features of

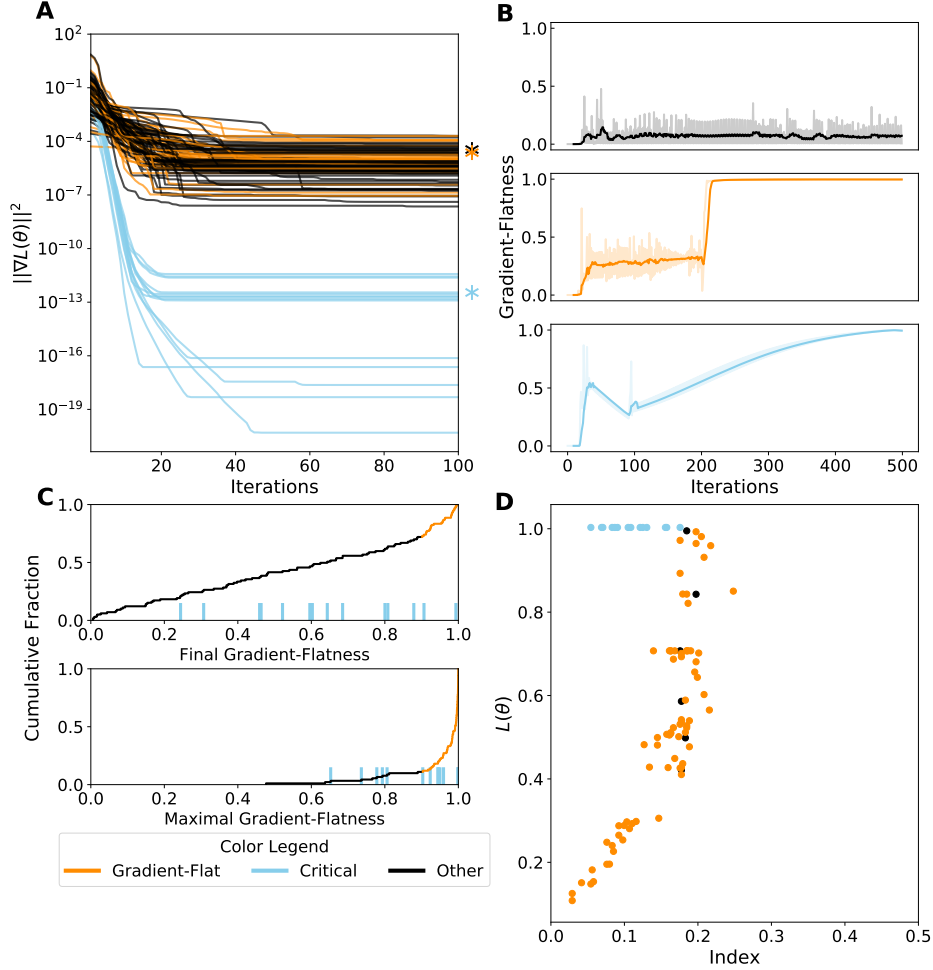


Figure 3: Critical Point-Finding Methods More Often Find Gradient-Flat Regions on a Neural Network Loss. **A:** Squared gradient norms across the first 100 iterations of Newton-MR for 100 separate runs on an auto-encoder loss. Gradient norms were flat after 100 iterations. See Appendix A.1 for details. Runs that terminate with squared gradient norm below $1e-10$, i.e. at a critical point, in blue. Runs that terminate above that cutoff and with r above 0.9, i.e. in a gradient-flat region, in orange. All other runs in black. Asterisks indicate trajectories in **B**. **B:** The relative residual norm r , an index of gradient-flatness, for the approximate Newton update computed by MR-QLP at each iteration (solid lines) for three representative traces. Values are local averages with a window size of 10 iterations. Raw values are plotted transparently underneath. Top: non-flat, non-critical point (black). Middle: flat, non-critical point (orange). Bottom: flat, critical point (blue). **C:** Empirical cumulative distribution functions for the final (top) and maximal (bottom) relative residual norm r observed during each run of Newton-MR. Values above the cutoff for approximate gradient-flatness, $r > 0.9$, in orange. Observations from runs that terminated below the cutoff for critical points, $\|\nabla L(\theta)\|^2 < 1e-10$, indicated with blue ticks. **D:** Loss and index for the maximally gradient-flat points obtained during application of Newton-MR. Points with squared gradient norm below $1e-10$ in blue. Other points colored by their gradient-flatness: points above 0.9 in orange, points below in black. Only points with squared gradient norm below $1e-4$ shown.

the loss-index relationship reported in [11] and [39] are recreated: convex shape, small spread at low index that increases for higher index, no minima or near-minima at high values of the loss. However, our analysis suggests that the majority of these points are not critical points but either strict gradient-flat points (orange) or simply points of spurious or incomplete Newton convergence (black). The approximately critical points we do see (blue) have a very different loss-index relationship: their loss is equal to the loss of a network with all parameters set to 0 and their index is low, but not 0.

4 Discussion

The results above and in the appendices demonstrate that gradient-flat regions, where the gradient is nearly in the approximate kernel of the Hessian, are a prevalent feature of some prototypical neural network loss surfaces and that many critical point-finding methods are attracted to them. The networks used in this paper are very small, relative to practical networks for image recognition and natural language processing, which have several orders of magnitude more parameters. However, increasing parameter count tends to increase the singularity of loss Hessians [44], and so we expect there to be even greater gradient-flatness for larger networks.

The strategy of using gradient norm cutoffs to determine whether a point is near enough to a critical point for the loss and index to match the true value is natural, but in the absence of guarantees on the smoothness of the behavior of the Hessian (and its spectrum) around the critical point, the numerical value sufficient to guarantee correctness is unclear. Our observations of gradient-flat regions at extremely low gradient norm and the separation of these values, in terms of loss-index relationship, from the bulk of the observations suggest that there may be spurious targets of convergence for critical point-finding methods even at such low gradient norm. Alternatively, they may in fact be near real critical points, and so indicate that the simple, convex picture of loss-index relationship painted by the numerical results in [11] and [39] is incomplete. Indeed, recent analytical results have demonstrated that bad local minima do exist for almost all neural network architectures and datasets (see [12] for a helpful table of positive and negative theoretical results regarding local minima). Furthermore, our observation of singular Hessians at low gradient norm suggests that some approximate saddle points of neural network losses may be degenerate (as defined in [23]) and non-strict (as defined in [29]), which indicates that gradient descent may be attracted to these points, according to the analyses in [23] and [29]. These points need not be local minima. However, in two cases we observe the lowest-index saddles at low values of the loss (see Fig. 3, Fig. A.1) and so these analyses still predict that gradient descent will successfully reduce the loss, even if it doesn't find a local minimum. In the third case, an over-parameterized network Fig. A.2, we do observe a bad local minimum, as predicted in [12] for networks capable of achieving 0 training error.

Our results motivate a revisiting of the numerical results in [11] and [39]. Looking back at Figure 4 of [11], we see that their non-convex Newton method, a second-order optimization algorithm designed to avoid saddle points by reversing the Newton update along directions of negative curvature, appears to terminate at a gradient norm of order 1. This is only a single order of magnitude lower than what was observed during training. It is likely that this point was either in a gradient-flat region or otherwise had sufficient gradient norm in the Hessian kernel to slow the progress of their algorithm. This observation demonstrates that second-order methods designed for optimization, which use the loss as a merit function, rather than norms of the gradient, can terminate in gradient-flat regions. In this case, the merit function encourages convergence to points where the loss, rather than the gradient norm, is small, but it still cannot guarantee convergence to a critical point. The authors of [11] do not report a gradient norm cutoff, among other details needed to recreate their critical point-finding experiments, so it is unclear to which kind of points they converged. If, however, the norms are as large as those of the targets of their non-convex Newton method, in accordance with our experience with damped Newton methods and that of [10], then the loss-index relationships reported in their Figure 1 are likely to be for gradient-flat points, rather than critical points.

The authors of [39] do report a squared gradient norm cutoff of $1e-6$. This cutoff is right in the middle of the bulk of values we observed, and which we labeled gradient-flat regions and points of spurious convergence, based on the cutoff in [16], which separates a small fraction of runs from this bulk. This suggests that some of their putative critical points were gradient flat points. Their Figure 6 shows a disagreement between

their predictions for the index, based on a loss-weighted mixture of a Wishart and Wigner random matrix, and their observations. We speculate that some of this gap is due to their method recovering approximate gradient-flat points rather than critical points.

Even in the face of results indicating the existence of bad local minima [12], it remains possible that bad local minima of the loss are avoided by initialization and optimization strategies. For example ReLU networks suffer from bad local minima when one layer’s activations are all 0, or when the biases are initialized at too small of a value [21], but careful initialization and training can avoid the issue. Our results do not directly invalidate this hypothesis, but they do call the supporting numerical evidence into question. Our observation of gradient-flat regions on almost every single run suggests that, while critical points are hard to find and may even be rare, regions where gradient norm is extremely small are neither. For non-smooth losses, e.g. those of ReLU networks or networks with max-pooling, whose loss gradients can have discontinuities, critical points need not exist, but gradient-flat regions may. Indeed, in some cases, the only differentiable minima in ReLU networks are also flat [27].

Other types of critical point-finding methods are not necessarily attracted to gradient-flat regions, in particular Newton homotopy methods (first used on neural networks in the 90s [10], then revived in the 2010s [3, 35]), which are popular in algebraic geometry [4]. However, singular Hessians still cause issues: for a singular Hessian H , the curve to be continued by the homotopy becomes a manifold with dimension $1 + \text{rank}(H)$, and orientation becomes more difficult. This can be avoided by removing the singularity of the Hessian, e.g. by the randomly-weighted regularization method in [34]. However, while these techniques may make it possible to find critical points, they fundamentally alter the loss surface, limiting their utility in drawing conclusions about other features of the loss. In particular, in the time since the initial resurgence of interest in the curvature properties of neural network losses sparked by [11], the importance of overparameterization for optimization of and generalization by neural networks has been identified [30, 40]. Large overparameterized networks have more singular Hessians [44], and so the difference between the original loss and an altered version with an invertible Hessian is greater. Furthermore the prevalence of gradient-flat regions should be greater, since the Hessian kernel covers an increasingly large subspace.

The authors of [44] emphasize that when the Hessian is singular everywhere, the notion of a basin of attraction is misleading, since targets of convergence form connected manifolds and some assumptions in theorems guaranteeing first-order convergence become invalid [23], though with sufficient, if unrealistic, overparameterization convergence can be proven [14]. They speculate that a better approach to understanding the behavior of optimizers focuses on their exploration of the sub-level sets of the loss. Our results corroborate that speculation and further indicate that this flatness means using second-order methods to try to accelerate exploration of these regions in search of minimizers is likely to fail: the alignment of the gradient with the Hessian’s approximate kernel will tend to produce extremely large steps, for some methods, or no acceleration and even convergence to non-minimizers, for others.

Our observation of ubiquitous gradient-flatness further provides an alternative explanation for the success and popularity of approximate second-order optimizers for neural networks, like K-FAC [32], which uses a layerwise approximation to the Hessian. These methods are typically motivated by appeals to the computational cost of even Hessian-free exact second-order methods and their brittleness in the stochastic (non-batch) setting. However, exact second-order methods are only justified when the second-order model is good, and at an exact gradient-flat point, the second-order model can be infinitely bad, in a sense, along the direction of the gradient. Approximations need not share this property. Even more extreme approximations, like the diagonal approximations in the adaptive gradient family (e.g. AdaGrad [15], Adam [26]), behave very reasonably in gradient-flat regions: they smoothly scale up the gradient in the directions in which it is small and changing slowly, without making a quadratic model that is optimal in a local sense but poor in a global sense.

Overall, our results underscore the difficulty of searching for critical points of singular non-convex functions, including deep network loss functions, and shed new light on other numerical results in this field. In this setting, second-order methods for finding critical points can fail badly, by converging to gradient-flat points. This failure can be hard to detect unless it is specifically measured. Furthermore, gradient-flat points are generally places where quadratic approximations become untrustworthy, and so our observations are of relevance for the design of exact and approximate second-order optimization methods as well.

Acknowledgements

The authors would like to thank Yasaman Bahri, Jesse Livezey, Dhagash Mehta, Dylan Paiton, and Ryan Zarcone for useful discussions. Authors CF & AL were supported by the National Science Foundation Graduate Research Fellowship Program under Grant No. DGE 1752814. NW was supported by the Google PhD Fellowship. Author AL was supported by a National Institutes of Health training grant, 5T32NS095939. MRD was supported in part by the U. S. Army Research Laboratory and the U. S. Army Research Office under contract W911NF-13-1-0390. KB was funded by a DOE/LBNL LDRD, ‘Deep Learning for Science’, (PI, Prabhat).

References

- [1] L. Angelani, R. Di Leonardo, G. Ruocco, A. Scala, and F. Sciortino. Saddles in the energy landscape probed by supercooled liquids. *Physical Review Letters*, 85(25):5356–5359, 2000.
- [2] Pierre Baldi and Kurt Hornik. Neural networks and principal component analysis: Learning from examples without local minima. *Neural Networks*, 2(1):53 – 58, 1989.
- [3] Andrew J. Ballard, Ritankar Das, Stefano Martiniani, Dhagash Mehta, Levent Sagun, Jacob D. Stevenson, and David J. Wales. Energy landscapes for machine learning. *Phys. Chem. Chem. Phys.*, 19:12585–12603, 2017.
- [4] Daniel J. Bates, Jonathan D. Haunstein, Andrew J. Sommes, and Charles W. Wampler. *Numerically Solving Polynomial Systems with Bertini (Software, Environments and Tools)*. Society for Industrial and Applied Mathematics, 2013.
- [5] Stephen Boyd and Lieven Vandenberghe. *Convex Optimization*. Cambridge University Press, New York, NY, USA, 2004.
- [6] Kurt Broderix, Kamal K. Bhattacharya, Andrea Cavagna, Annette Zippelius, and Irene Giardina. Energy landscape of a Lennard-Jones liquid: statistics of stationary points. *Physical Review Letters*, 85(25):5360–5363, 2000.
- [7] Richard H. Byrd, Marcelo Marazzi, and Jorge Nocedal. On the convergence of newton iterations to non-stationary points. *Mathematical Programming*, 99(1):127–148, January 2004.
- [8] Charles J. Cerjan and William H. Miller. On finding transition states. *The Journal of Chemical Physics*, 75(6):2800–2806, September 1981.
- [9] Sou-Cheng T. Choi, Christopher C. Paige, and Michael A. Saunders. MINRES-QLP: A Krylov subspace method for indefinite or singular symmetric systems. *SIAM Journal on Scientific Computing*, 33(4):1810–1836, 2011.
- [10] Frans Coetzee and Virginia L. Stonick. 488 solutions to the XOR problem. In M. C. Mozer, M. I. Jordan, and T. Petsche, editors, *Advances in Neural Information Processing Systems 9*, pages 410–416. MIT Press, 1997.
- [11] Yann Dauphin, Razvan Pascanu, Çağlar Gülçehre, Kyunghyun Cho, Surya Ganguli, and Yoshua Bengio. Identifying and attacking the saddle point problem in high-dimensional non-convex optimization. *CoRR*, abs/1406.2572, 2014.
- [12] Tian Ding, Dawei Li, and Ruoyu Sun. Sub-optimal local minima exist for almost all over-parameterized neural networks. 2019.
- [13] Jonathan P. K. Doye and David J. Wales. Saddle points and dynamics of Lennard-Jones clusters, solids, and supercooled liquids. *The Journal of Chemical Physics*, 116(9):3777–3788, 2002.
- [14] Simon S. Du, Xiyu Zhai, Barnabas Poczos, and Aarti Singh. Gradient descent provably optimizes over-parameterized neural networks. In *International Conference on Learning Representations*, 2019.

- [15] John Duchi, Elad Hazan, and Yoram Singer. Adaptive subgradient methods for online learning and stochastic optimization. *J. Mach. Learn. Res.*, 12(null):2121–2159, July 2011.
- [16] Charles G. Frye, Neha S. Wadia, Michael R. DeWeese, and Kristofer E. Bouchard. Numerically recovering the critical points of a deep linear autoencoder, 2019.
- [17] Timur Garipov, Pavel Izmailov, Dmitrii Podoprikin, Dmitry Vetrov, and Andrew Gordon Wilson. Loss surfaces, mode connectivity, and fast ensembling of dnns, 2018.
- [18] Behrooz Ghorbani, Shankar Krishnan, and Ying Xiao. An investigation into neural net optimization via hessian eigenvalue density, 2019.
- [19] Ian J. Goodfellow and Oriol Vinyals. Qualitatively characterizing neural network optimization problems. *CoRR*, abs/1412.6544, 2014.
- [20] A. Griewank and M. R. Osborne. Analysis of Newton’s method at irregular singularities. *SIAM Journal on Numerical Analysis*, 20(4):747–773, 1983.
- [21] David Holzmüller and Ingo Steinwart. Training two-layer relu networks with gradient descent is inconsistent, 2020.
- [22] Alexey F. Izmailov and Mikhail V. Solodov. *Newton-Type Methods for Optimization and Variational Problems*. Springer International Publishing, 2014.
- [23] Chi Jin, Rong Ge, Praneeth Netrapalli, Sham M. Kakade, and Michael I. Jordan. How to escape saddle points efficiently. *CoRR*, abs/1703.00887, 2017.
- [24] Chi Jin, Lydia T. Liu, Rong Ge, and Michael I. Jordan. Minimizing nonconvex population risk from rough empirical risk. *CoRR*, abs/1803.09357, 2018.
- [25] Chi Jin, Praneeth Netrapalli, and Michael I. Jordan. Accelerated gradient descent escapes saddle points faster than gradient descent. In Sébastien Bubeck, Vianney Perchet, and Philippe Rigollet, editors, *Proceedings of the 31st Conference On Learning Theory*, volume 75 of *Proceedings of Machine Learning Research*, pages 1042–1085. PMLR, 2018.
- [26] Diederik P. Kingma and Jimmy Ba. Adam: A method for stochastic optimization, 2014.
- [27] Thomas Laurent and James von Brecht. The multilinear structure of relu networks, 2017.
- [28] Yann LeCun, Corinna Cortes, and CJ Burges. Mnist handwritten digit database. *ATT Labs [Online]*. Available: <http://yann.lecun.com/exdb/mnist>, 2, 2010.
- [29] Jason D. Lee, Max Simchowitz, Michael I. Jordan, and Benjamin Recht. Gradient descent only converges to minimizers. In Vitaly Feldman, Alexander Rakhlin, and Ohad Shamir, editors, *29th Annual Conference on Learning Theory*, volume 49 of *Proceedings of Machine Learning Research*, pages 1246–1257, Columbia University, New York, New York, USA, 2016. PMLR.
- [30] Dawei Li, Tian Ding, and Ruoyu Sun. On the benefit of width for neural networks: Disappearance of bad basins, 2018.
- [31] Dougal Maclaurin. *Modeling, Inference and Optimization with Composable Differentiable Procedures*. PhD thesis, Harvard University, April 2016.
- [32] James Martens and Roger Grosse. Optimizing neural networks with kronecker-factored approximate curvature, 2015.
- [33] James W. McIver and Andrew Komornicki. Structure of transition states in organic reactions. general theory and an application to the cyclobutene-butadiene isomerization using a semiempirical molecular orbital method. *Journal of the American Chemical Society*, 94(8):2625–2633, 1972.

- [34] Dhagash Mehta, Tianran Chen, Tingting Tang, and Jonathan D. Hauenstein. The loss surface of deep linear networks viewed through the algebraic geometry lens, 2018.
- [35] Dhagash Mehta, Xiaojun Zhao, Edgar A. Bernal, and David J. Wales. Loss surface of XOR artificial neural networks. *Physical Review E*, 97(5), 2018.
- [36] Jorge Nocedal and Stephen J. Wright. *Numerical optimization*. Springer series in operations research and financial engineering. Springer, New York, NY, 2. ed. edition, 2006.
- [37] Adam Paszke, Sam Gross, Francisco Massa, Adam Lerer, James Bradbury, Gregory Chanan, Trevor Killeen, Zeming Lin, Natalia Gimelshein, Luca Antiga, et al. Pytorch: An imperative style, high-performance deep learning library. In *Advances in Neural Information Processing Systems*, pages 8024–8035, 2019.
- [38] F. Pedregosa, G. Varoquaux, A. Gramfort, V. Michel, B. Thirion, O. Grisel, M. Blondel, P. Prettenhofer, R. Weiss, V. Dubourg, J. Vanderplas, A. Passos, D. Cournapeau, M. Brucher, M. Perrot, and E. Duchesnay. Scikit-learn: Machine learning in Python. *Journal of Machine Learning Research*, 12:2825–2830, 2011.
- [39] Jeffrey Pennington and Yasaman Bahri. Geometry of neural network loss surfaces via random matrix theory. In *International Conference on Learning Representations (ICLR)*, 2017.
- [40] Tomaso Poggio, Qianli Liao, and Andrzej Banburski. Complexity control by gradient descent in deep networks. *Nature Communications*, 11(1), February 2020.
- [41] Michael JD Powell. A hybrid method for nonlinear equations. *Numerical methods for nonlinear algebraic equations*, 1970.
- [42] Prajit Ramachandran, Barret Zoph, and Quoc V. Le. Searching for activation functions, 2017.
- [43] Fred Roosta, Yang Liu, Peng Xu, and Michael W. Mahoney. Newton-MR: Newton’s method without smoothness or convexity, 2018.
- [44] Levent Sagun, Utku Evci, V. Ugur Güney, Yann Dauphin, and Léon Bottou. Empirical analysis of the Hessian of over-parametrized neural networks. *CoRR*, abs/1706.04454, 2017.
- [45] Gilbert Strang. The fundamental theorem of linear algebra. *The American Mathematical Monthly*, 100(9):848, November 1993.
- [46] Ruoyu Sun. Optimization for deep learning: theory and algorithms, 2019.
- [47] Chiyuan Zhang, Samy Bengio, Moritz Hardt, Benjamin Recht, and Oriol Vinyals. Understanding deep learning requires rethinking generalization. *CoRR*, abs/1611.03530, 2016.

A Appendices

A.1 Networks and Datasets

A.1.1 Datasets

For the experiments in Fig. 1, 10000 16-dimensional Gaussian vectors with mean parameter 0 and diagonal covariance with linearly-spaced values between 1 and 16 were generated and then mean-centered.

For the experiments in Fig. 3 and Fig. A.1, 10000 images from the MNIST dataset [28] were cropped to 20 x 20 and rescaled to 4 x 4 using PyTorch [37], then z -scored. This was done for two reasons. Firstly, to improve the conditioning of the data covariance, which is very poor for MNIST due to low variance in the border pixels. Secondly, to reduce the number of parameters n in the network, as computing a high-quality inexact Newton solution is $O(n^2)$. Non-linear classification networks trained on this down-sampled data could still obtain accuracies above 90%, better than the performance of logistic regression ($\approx 87\%$).

For the experiments in Fig. A.2, 50 random images of 0s and 1s from the MNIST dataset were PCA-downsampled to 32 dimensions using sklearn [38]. This provided an alternative approach to improving the conditioning of the data covariance and reducing the parameter counts in the network. The labels for these images were then shuffled.

A.1.2 Networks

All networks, their optimization algorithms, and the critical point-finding algorithms were defined in the `autograd` Python package [31]. For the experiments in Fig. 1, two networks were trained: a linear auto-encoder with a single, fully-connected hidden layer of 4 units and a deep non-linear auto-encoder with two fully-connected hidden layers of 16 and 4 units with Swish [42] activations. Performance of the critical point-finding algorithms was even worse for networks with rectified linear units (results not shown) as reported by others (Pennington and Bahri, personal communication). Non-smooth losses need not have gradients that smoothly approach 0 near local minimizers, so it is only sensible to apply critical point-finding to smooth losses, see [27]. The non-linear auto-encoder used ℓ_2 regularization. Neither network had biases. All auto-encoding networks were trained with mean squared error.

For the experiments in Fig. 3, a fully-connected autoencoder with two hidden layers of 8 and 16 units, with Swish activations and biases, was used. This network had no ℓ_2 regularization.

For the experiments in Fig. A.1, a fully-connected classifier with two hidden layers of 12 and 8 units, with Swish activations and biases, was used. This network had ℓ_2 regularization, since the cross-entropy loss with which it was trained can otherwise have critical points at infinity.

For the experiments in Fig. A.2, a fully-connected classifier with two hidden layers of 32 and 4 units, with Swish activations, was used. This network had no biases. This network also used ℓ_2 regularization and was trained with the cross entropy loss. Networks were trained to near-perfect training performance: 48 to 50 correctly-classified examples out of 50.

A.2 Critical Point-Finding Experiments

For all critical point-finding experiments, we followed the basic procedure pioneered in [11] and used in [39] and [16]. First, an optimization algorithm was used to train the network multiple times. For the results in Fig. 1, this algorithm was full-batch gradient descent, while for the remainder of the results, this algorithm was full-batch gradient descent with momentum (learning rates 0.1 in both cases; momentum 0.9 in the latter).

The parameter values produced during optimization were then used as starting positions for Newton-MR. Following [39] and based on the arguments in [16], we selected these initial points uniformly at random with respect to their loss value.

Newton-MR [43] computes an inexact Newton update with the MR-QLP solver [9] and then performs back-tracking line search based on the squared gradient norm. For pseudocode of the equivalent exact algorithm, see Appendix A.3

The MR-QLP solver has the following hyperparameters for determining stopping behavior: maximum number of iterations (`maxit`), maximum solution norm (`maxxnorm`), relative residual tolerance (`rtol`), condition number limit (`acondlim`). We set `maxit` to be equal to the number of parameters, since with exact arithmetic, this is sufficient to solve the Newton system. We found that the `maxxnorm` and `acondlim` parameters did not affect stopping behavior, which was driven by the tolerance `rtol`. For Fig. 1, we used a tolerance of $1e-10$. For Fig. 3 and Fig. A.1, we used a tolerance of $5e-4$, based on the values for the relative residuals found after `maxit` iterations on test points. See Appendix A.4 for details about the relative residual stopping criterion. We do not provide pseudocode for this algorithm; see [9].

The back-tracking line search has the following hyperparameters: α , the starting step size, β , the multiplicative factor by which the step size is reduced, and ρ , the degree of improvement required to terminate the line search. We set these hyperparameters to $\alpha := 0.1$, $\beta := 0.5$, and $\rho := 0.1$. Furthermore, in back-tracking line search for Newton methods, it is important to always check a unit step size in order to attain supralinear convergence [36]. So before running the line search, we also check unit step size with a stricter $\rho' := 0.5$.

A.3 Newton-MR Pseudocode

Algorithm 1: Exact Newton-MR

Require $T \in \mathbb{N}, \theta_0 \in \mathbb{R}^N,$
 $\nabla f: \mathbb{R}^N \rightarrow \mathbb{R}^N, \nabla^2 f: \mathbb{R}^N \rightarrow \mathbb{R}^{N \times N}$

$t = 0$

while $t < T$ **do**

$g \leftarrow \nabla f(\theta_t)$

$H \leftarrow \nabla^2 f(\theta_t)$

$P \leftarrow \arg \min_{p'} \|Hp' + g\|^2$

$p \leftarrow \underset{p \in P}{\operatorname{argmin}} \|p\|^2$

$\alpha \leftarrow \arg \min_{\alpha} \|\nabla f(\theta_t + \alpha p)\|^2$

$\theta_{t-1} \leftarrow \theta_t + \alpha p$

if $\theta_t = \theta_{t-1}$ **then**

break

end

$t \leftarrow t + 1$

end

The pseudocode in Algorithm 1 defines an exact least-squares Newton method with exact line search. To obtain the inexact Newton-MR algorithm, the double argmin to determine the update direction p should be approximately satisfied using the MR-QLP solver [9] and the argmin to determine the step size α should be approximately satisfied using Armijo-type back-tracking line search. For details, see [43].

A.4 Relative Residual and Relative Co-Kernel Residual

The relative residual norm, r , measures the size of the error of an approximate solution to the Newton system. Introducing the symbols H and g , for the Hessian and gradient at a query point, the Newton system may be written $0 = Hp + g$ and r is then

$$r(p) = \frac{\|Hp + g\|}{\|H\|_F \|p\| + \|g\|}$$

where $\|M\|_F$ of a matrix M is its Frobenius norm.

Since all quantities are non-negative, r is non-negative; because the denominator bounds the numerator, by the triangle inequality and the compatibility of the Frobenius and Euclidean norms, r is at most 1. For an exact solution of the Newton system p^* , $r(p^*)$ is 0, the minimum value, while $r(0)$ is 1, the maximum value. Note that small values of $\|p\|$ do not imply large values of this quantity, since $\|p\|$ goes to 0 when a Newton method converges towards a critical point, while r goes to 0.

When g is partially in the kernel of H , the Newton system is unsatisfiable, as g will also be partly in the co-image of H , the linear subspace into which H cannot map any vector. In this case, the minimal value for r will no longer be 0. The optimal solution for $\|Hp + g\|$ instead has the property that its residual is 0 once restricted to the co-kernel of H , the linear subspace orthogonal to the kernel of H . This co-kernel residual can be measured by applying the matrix H to the residual vector $Hp + g$. After normalization, it becomes

$$r_H(p) = \frac{\|H(Hp + g)\|}{\|H\|_F \|Hp + g\|}$$

Note that this value is also small when the gradient lies primarily along the eigenvalues of smallest magnitude. On each internal iteration, MR-QLP checks whether either of these values is below a tolerance level – in our experiments, $5e-4$ – and if either is, it ceases iteration. With exact arithmetic, either one or the other of these values should go to 0 within a finite number of iterations; with inexact arithmetic, they should just become small. See [9] for details. Less than 5% of Newton steps were obtained from the kernel residual going below the tolerance, indicating that almost all points of the loss surface had an approximately unsatisfiable Newton system.

A.5 Replication of Results from Sec. 3 on MNIST MLP

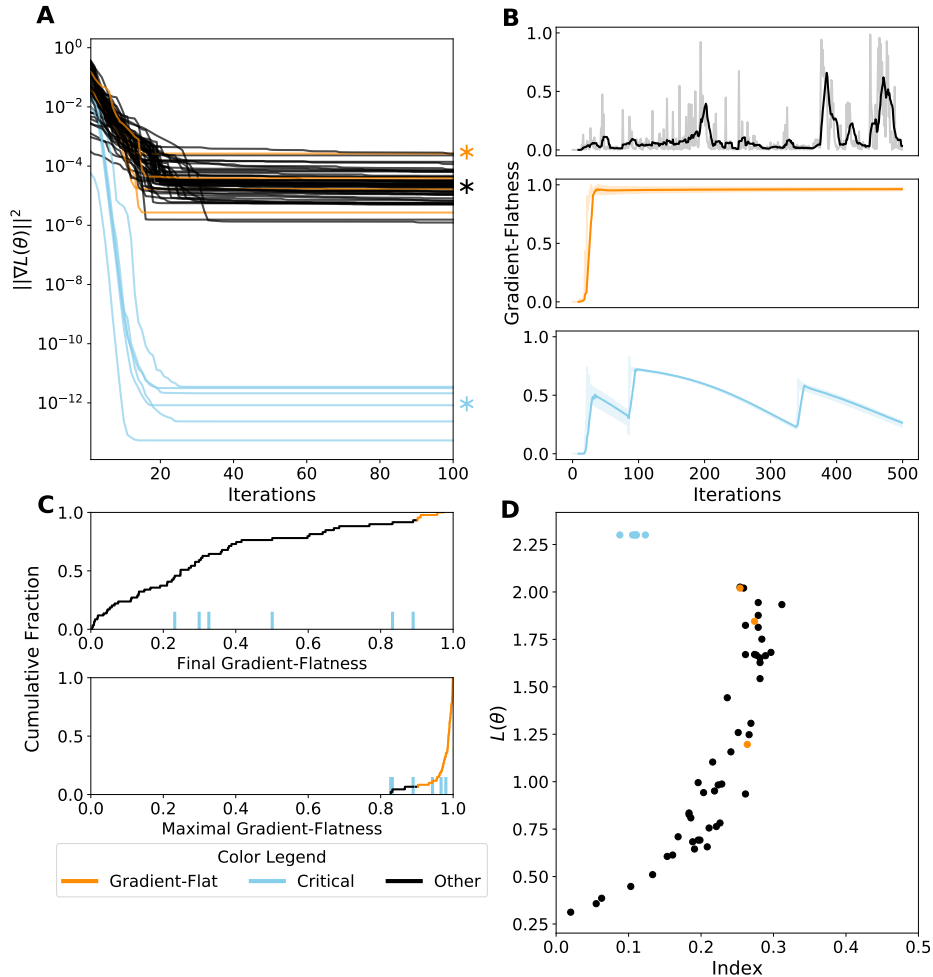


Figure A.1: **Gradient-Flat Regions Also Appear on an MLP Loss.** **A:** Squared gradient norms across the first 100 iterations of Newton-MR for 60 separate runs on an MLP loss (see Appendix A.1 for details). Runs that terminate with squared gradient norm below 10^{-10} in blue. Runs that terminate above that cutoff and with r above 0.9, in orange. All other runs in black. Asterisks indicate trajectories in **B**. **B:** The relative residual norm r , for the approximate Newton update computed by MR-QLP at each iteration for three representative traces. Values are local averages with a window size of 10 iterations. Raw values are plotted transparently underneath. Top: non-flat, non-critical point (black). Middle: flat, non-critical point (orange). Bottom: non-flat, critical point (blue). **C:** Empirical cumulative distribution functions for the final (top) and maximal (bottom) relative residual norm r . Values above the cutoff for approximate gradient-flatness, $r > 0.9$, in orange. Observations from runs that terminated below the cutoff for critical points, $\|\nabla L(\theta)\|^2 < 10^{-10}$, indicated with blue ticks. **D:** Loss and index for the points found after 500 iterations of Newton-MR. Colors as in top-left; only points with squared gradient norm below 10^{-4} shown.

We repeated the experiments whose results are visualized in Fig. 3 on the loss surface of a fully-connected classifier on the same modified MNIST dataset (details in Appendix A.1). We again found that the performance of the Newton-MR critical point-finding algorithm was poor (Fig. A.1A) and that around 90% of runs encountered a point with gradient-flatness above 0.9 (Fig. A.1C, bottom row). However, we observed that fewer runs terminated at a gradient-flat point (Fig. A.1C, top row), perhaps because the algorithm was bouncing in and out of gradient-flat regions (Fig. A.1B, top and bottom rows), rather than because of another type of spurious Newton convergence. If we measure the loss-index relationship at these non-gradient-flat points (Fig. A.1D), we see the same pattern as in Fig. 3. This also holds if we look at the maximally flat points, as in Fig. 3D (results not shown).

A.6 Replication of Results from Sec. 3 on Binary MNIST Subset Memorization

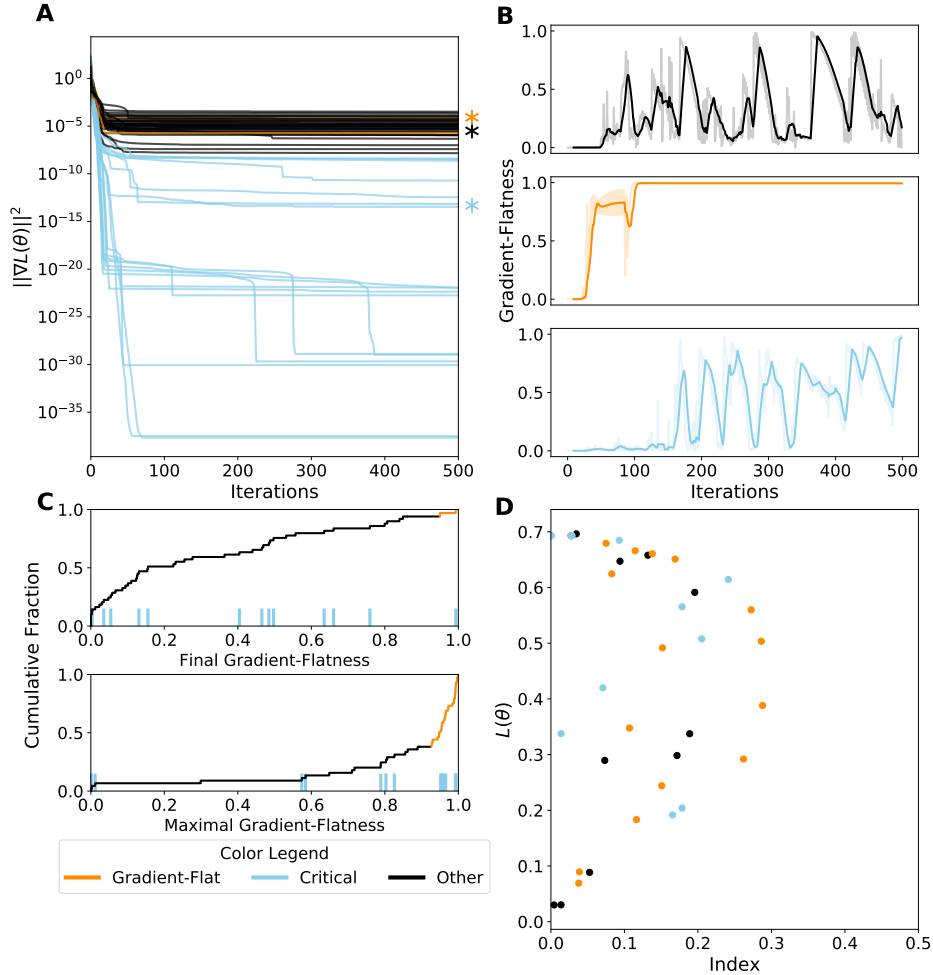


Figure A.2: **Gradient-Flat Regions Also Appear on an Over-Parameterized Loss.** **A:** Squared gradient norms across 500 iterations of Newton-MR for 50 separate runs on the loss of an over-parameterized network (see Appendix A.1 for details). Runs that terminate with squared gradient norm below $1e-10$ in blue. Runs that terminate above that cutoff and with r above 0.9, in orange. All other runs in black. Asterisks indicate trajectories in **B**. **B:** The relative residual norm r , for the approximate Newton update computed by MR-QLP at each iteration for three representative traces. Values are local averages with a window size of 10 iterations. Raw values are plotted transparently underneath. Top: non-flat, non-critical point (black). Middle: flat, non-critical point (orange). Bottom: flat, critical point (blue). **C:** Empirical cumulative distribution functions for the final (top) and maximal (bottom) relative residual norm r . Values above the cutoff for approximate gradient-flatness, $r > 0.9$, in orange. Observations from runs that terminated below the cutoff for critical points, $\|\nabla L(\theta)\|^2 < 1e-10$, indicated with blue ticks. **D:** Loss and index for the points found after 500 iterations of Newton-MR. Colors as in top-left; only points with squared gradient norm below $1e-4$ shown.

We repeated the experiments whose results are visualized in Fig. 3 on the loss surface of a fully-connected classifier on a small subset of 50 0s and 1s from the MNIST dataset (details in Appendix A.1). In this setting, the network is over-parameterized, in that it has a hidden layer almost as wide as the number of points in the dataset (32 vs 50) and has more parameters than there are points in the dataset (1160 vs 50). It is also capable of achieving 100% accuracy on this training set, which has random labels, as in [47]. We again observe that the majority of runs do not terminate with squared gradient norm under $1e-8$ (33 out of 50 runs) and a similar fraction (31 out of 50 runs) encounter gradient-flat points (Fig. A.2A and C, bottom panel). The loss-index relationship looks qualitatively different, as might be expected for a task with random labels. Notice the appearance of a bad local minimum: the blue point at index 0 and loss $\ln(2)$.